International Journal of Lightweight Materials and Manufacture 6 (2023) 117–128

Contents lists available at ScienceDirect

International Journal of Lightweight Materials and Manufacture

journal homepage: www.keaipublishing.com/ijlmm

Original Article

Mechanical and thermal properties of graphene nanoplatelets-reinforced recycled polycarbonate composites

Devinda Wijerathne [a], Youyun Gong [b], Shaila Afroj [c, d], Nazmul Karim [c, d], Chamil Abeykoon [b, *]

[a] Department of Mechanical Engineering, Faculty of Engineering, University of Peradeniya, Peradeniya, Sri Lanka
[b] Aerospace Research Institute and Northwest Composites Centre, Department of Materials, Faculty of Science and Engineering, The University of Manchester, Oxford Road, M13 9PL, Manchester, UK
[c] National Graphene Institute (NGI), Faculty of Science and Engineering, The University of Manchester, Oxford Road, M13 9PL, Manchester, UK
[d] Centre for Print Research (CFPR), University of the West of England, Frenchay, Bristol BS16 1QY, UK

ARTICLE INFO

Article history:
Received 18 May 2022
Received in revised form
31 August 2022
Accepted 1 September 2022
Available online 7 September 2022

Keywords:
Polymer nanocomposites
Graphene nanoplatelets
Virgin/recycled polycarbonate
Processing parameters
Thermal/mechanical properties

ABSTRACT

Nanocomposites have received significant interest in recent years, as they offer improved properties compared to conventional materials for various applications. Among many available nanofillers, graphene nanoplatelets (GNP) have shown promising results for polymer-based nanocomposite applications. This paper investigates the mechanical and thermal properties of GNP-reinforced virgin and recycled polycarbonate (PC) nanocomposites blended *via* a twin-screw extruder. Effects of various key processing parameters such as filler concentration, processing speed, barrel/die set temperature, and PC type (virgin and recycled) on the reinforced composites were examined. Mechanical properties were characterised by tensile testing, while thermogravimetric analysis (TGA) and differential scanning calorimetry (DSC) were used to characterise the thermal properties. The results show that the processing speed and barrel/die set temperature have a slight influence, while the filler concentration significantly affects the properties of PC/GNPs composites. The Young's modulus and yield strength were enhanced with increasing GNP loading, where the maximum enhancement of Young's modulus was obtained as ~33% for virgin-PC/GNP and ~39.5% for recycled-PC/GNP composites at 10 wt.-% GNP loading. However, the failure strain was reduced with the increased GNP loading for both virgin and recycled PC/GNP composites. Embedding GNP into the PC matrix only slightly influenced the thermal stability and glassy transition temperature (T_g). The highest thermal stability for virgin PC/GNP composites was observed with 1 wt.-% (2.74% increase with respect to virgin PC), while for recycled PC/GNP, it was observed with 10 wt.-% (2.42% increase with respect to recycled PC) GNP loading. Under the same GNP loading, recycled PC-based composites showed lower thermal stability than virgin PC-based composites. The T_g evaluated from DSC showed a rise under 1 wt.-% GNP for virgin PC/GNP and decrease afterwards with higher filler loading, while an irregular variation for recycled PC/GNP was observed.

1. Introduction

Materials are key components in many scientific fields. The demand for new materials with enhanced properties has increased exponentially over the years. To meet such growing demand, composite materials are being made by combining two or more existing materials. In the past few decades, polymers have gained significant interest as dominant matrix materials for composites due to their low cost, reproducibility [1], ease of processing [2], and so forth. Polymer nanocomposites are a special type of composite materials that are formed by embedding different nano units (fillers) within the polymer matrix [3–5] and are used in a wide range of applications [6–12].

In polymer nanocomposites, fillers are the most widely used additives to improve mechanical, electrical, and thermal properties. The global polymer filler market was ~US$ 50.3 billion in 2020 and

* Corresponding author.
E-mail address: chamil.abeykoon@manchester.ac.uk (C. Abeykoon).
Peer review under responsibility of Editorial Board of International Journal of Lightweight Materials and Manufacture.

https://doi.org/10.1016/j.ijlmm.2022.09.001

is predicted to increase over ~US$ 57.9 billion by 2026 [13]. Among the vast selection of fillers, carbonaceous nanofillers such as carbon nanofibers, graphite oxide, carbon nanotubes, and graphene nanoplatelets play a promising role due to their better structural and functional properties [5,7,14–18]. Graphene, first isolated in 2004 [19], has gained significant interest for multiple applications, including composites [20–22], membranes [23], flexible electronics [24,25], sensors [26], biomedical [27,28] and energy [29], due to its superior physical (2630 m2 g^{-1} of calculated specific surface area) [30], mechanical (~1 TPa of Young's modulus and ~130 GPa of tensile strength) [31], thermal (~5 × 10^3 W m^{-1} K^{-1} of thermal conductivity) [32] and electrical properties [33,34]. This interest is further improved by relatively lower production cost [35–37] and mass producibility [38,39] of graphene, where investigations were made on reinforcement with different types of polymers [40–48].

Graphene nanoplatelet is a 2D graphite material having a thickness of less than 100 nm [49], which contains closely packed graphene layers bonded *via* weak Van der Waals forces. Having the thickness in the nanometres range [49] and diameter in the micrometres range [50], GNP attains a high specific surface area [30,51] and high aspect ratio [50,52] as a nanofiller. GNP-based composites have shown better reinforcements at very low concentrations [42,43,53–55], indicating it as an effective functional modifier. The addition of a small amount of graphene-based materials can improve Young's modulus and tensile strength of composites [56,57]. Moreover, graphene-based polymer nanocomposites have shown better mechanical, thermal, rheological, and electrical properties in comparison to other conventional or carbonaceous nanofiller-based polymer composites [54,58–62]. Wang et al. [54] reported better tensile and impact strength with GNP-based high-density polyethylene (HDPE) nanocomposite than HDPE/carbon black nanocomposite. Yasmin et al. [59] compared the reinforcing effect of GNP and nanoclay in epoxy matrix and elaborated that a higher elastic modulus can be obtained with GNP as nanofillers. Similarly, Gupta et al. [60] reported significant improvement in storage modulus, loss modulus, and glass transition temperature of GNP-based vinyl ester-based nanocomposites [47]. Kalaitzidou et al. [62] have reported superior dimensional stability, and rheological behaviour with exfoliated graphite nanoplatelets reinforced polypropylene (PP) compared to the carbon black, nanoclay and carbon fibre reinforced PP. A study by Ramanathan et al. [58] on graphitic nanofiller-based poly (methyl methacrylate) (PMMA) nanocomposites reports superior mechanical, thermal and electrical properties for PMMA/GNP nanocomposites than other nanofillers-based (as received graphite and expanded graphite) nanocomposite. Moreover, they have elaborated that GNP has dispersed well within the polymer matrix due to its smaller size and higher surface area, resulting in property improvements. Similar findings have been reported [53,63–65], where a better reinforcing effect was observed due to the good dispersion of GNP in the polymer matrix. Furthermore, the high aspect ratio of GNP [66–69], better intercalation and interface bonding with polymer matrix [70] are also governing factors for better reinforcements in GNP-based nanocomposites.

Since good dispersion is a dominant factor for better reinforcement, the dispersion technique of GNP into the polymer matrix has become an essential part of nanocomposite characterisation. The intermolecular interactions such as Van der Walls [71], hydrophobic-hydrophobic [71] and π–π stacking [71] will enable bonding between GNP and polymer chains but obstruct the effective connection between two parties. Thus, in general, it has been reported that the polymer/GNP composites are heterogeneous mixtures [44,45]. Therefore, selecting appropriate processing techniques is vital to achieving good uniformity and degree of dispersion. The most common processing methods in polymer composites processing are solution blending [71–73], in-situ polymerisation [74] and melt blending [5,75–77]. Solution blending and in-situ polymerisation offer better mixing between polymer and GNP [59,70,78,79] due to the porous nature of GNP [80,81]. However, these two techniques are less favourable in industrial-level production due to the involvement of hazardous chemicals and high production costs [36,82]. On the other hand, limitations of melt blending are reported as a relatively low degree of dispersion [83,84], reduction in the aspect ratio of the nanofillers [85], dependency on the equipment type, geometry, and operating conditions [86]. However, the melt blending approach is more popular in the polymer composites industry due to the low production cost and scalability [87] despite the limitations mentioned above. Melt blending is commonly performed using extruders. Among the different selections of extruders, the twin screw extruder has proven to deliver the best results for polymer nanocomposites [83,88,89]. Therefore, a twin screw extruder was used to process PC/GNP nanocomposites in this study.

Polycarbonate (PC) is one of the most popular plastics, which has found a wide range of applications in automotive, aeronautical, electrical, photonics and construction industries [90–93]. Due to the good mechanical (stiffness of 2.0–2.4 GPa [90], unbreakable under unnotched condition [93]) and heat resistive properties (glass transition temperature ~ 150 °C and heat deflection temperature of 131 °C) [93], dimensional stability (coefficient of thermal expansion (28–80 °C) of 7 × 10^{-5} K^{-1}) [93] and optical transparency (refractive index of 1.59 and above 80% invisible spectrum) [90,93], PC has become popular in the nanocomposite industry over recent years. Lago et al. [73] studied PC-based graphene composites prepared using a solution blending method. A composite containing 1 wt.-% graphene flakes reported a ~26% increment in Young's modulus, while a ~10% increase in ultimate tensile strength was obtained with 2.5 wt.-% graphene flakes compared to the pristine PC used. Oyarzabal et al. [94] prepared PC/GNP nanocomposites dispersing untreated GNP through a melt blending method and reported a relative increment (compared to neat PC) of ~52% in elastic modulus with 7 wt.-% GNP loading. Similar behaviour has been published by King et al. [95], where the elastic modulus has been enhanced by ~9% and ~50% for PC/GNP nanocomposites prepared by melt blending with GNP contents of 3 and 7 wt.-%, respectively. Shen et al. [96] researched interfacial interaction between PC and thermally reduced graphene (TRG) induced by the combination of solution mixing and melt blending methods. They observed a ~6.5% improvement in tensile strength and a ~6.8% increment in Young's modulus in PC/graphene composites made with 10-minutes of melt mixing time compared to the composites made with zero melt mixing time.

Polycarbonate contains bisphenol-A, which makes it an environmentally harmful material [97–99]. Thus, the environmental impact of PC has become a hot topic where a growing concern can be seen in the current practices of PC disposal [97,99]. Therefore, an uptrend is forming to recycle PC [100] and use them in manufacturing industries [101–104]. Comparative to virgin PC, recycled PC has shown poor properties alike other recycled materials [101,105]. Despite having substandard properties, only a limited number of studies have aimed to improve recycled PC properties. The main methods that are being reported involve blending with other polymers [103,106,107] and the addition of fillers [103,108–113]. Therefore, our study is designed to widen the understanding of nanofiller reinforcement capability for the

property enhancement of recycled PC. Lorenzo et al. [112] have investigated recovered PC matrix nanocomposites filled with organic modified montmorillonites and have reported that increasing the nanoclay content can sometimes lead to a deterioration of the mechanical properties. Moreover, their results suggest that the mechanical properties of the recovered PC-based nanocomposites can only be improved if the molar mass of the PC remains above some critical value after processing. Glass fibre reinforced post-consumer PC has been studied by Al-Mulla and Gupta [110]. Their findings show that mechanical and flow properties of PC with 25% impurities blends with 15 wt.-% short glass fibre are indistinguishable from the corresponding properties of virgin PC with the same glass fibre content indicating that glass fibre can significantly improve the mechanical and rheological properties of recycled PC. However, the reinforcement capacity of nanofiller on recycled PC has not been presented sufficiently in the literature. Therefore, our study is designed to widen the understanding of nanofiller reinforcement capability for the property enhancement of recycled PC.

This study investigates the mechanical and rheological properties of virgin and recycled PC reinforced with GNP. The composites were processed using a twin screw extruder under four operating conditions (see Section 2.2). The effects of various key processing parameters such as filler concentration, processing speed and barrel/die set temperature on the composite properties were experimentally determined and analysed. To the knowledge of the authors, only a very limited number of previous studies have been reported so far by investigating the properties of recycled PC/GNPs composites; hence this work should be useful in understanding the performance of both virgin and recycled PC matrix with nanofillers.

2. Methodology

2.1. Materials

Exfoliated graphene nanoplatelets (M15 grade) with average particle diameters of 5, 15 and 25 μm, a typical surface area of 120–150 m^2/g and average thicknesses in the range of 6–8 nm were purchased from XG Sciences Inc. (Lansing, Michigan, USA) and used for this study. The matrix polymer, Makrolon grade polycarbonate and recycled polycarbonate were obtained through Covestro (Germany), and the essential specifications of the virgin PC are listed in Table 1.

2.2. Preparation of nanocomposites

Melt mixing process was used to process PC/GNPs (both virgin and recycled PC) nanocomposites *via* Haake MiniLab micro twin-screw compounder (Thermo Fisher Scientific, USA), which can provide good mixing over a broad range of processing conditions [88]. The formulation of the nanocomposites processed in this study is shown in Table 2. The extruder was operated at two temperatures (280 °C and 300 °C) and two speeds (50 rpm and 100 rpm) in order to create four different process conditions (50 rpm at 280 °C, 50 rpm at 300 °C, 100 rpm at 280 °C and 100 rpm at 300 °C).

Table 1
Main features of the virgin PC used for experiments.

Specific gravity, solid	1.2
Melt-flow rate (g/10 min)	3.0 (300 °C/1.2 kg)
Glass transition temperature (°C) at 10 °C/min	146
Supplier	Covestro, Germany

Table 2
The formulation of polymers and nanomaterials.

Nanocomposite sample	1	2	3	4	5	6
Sample name	GNP-0	GNP-1	GNP-3	GNP-5	GNP-8	GNP-10
PC (wt.-%)	100	99	97	95	92	90
GNP (wt.-%)	0	1	3	5	8	10

A maximum weight of 3 g of the mixture of PC/GNP was used for each processing condition to operate below the extruder capacity (7 cc), and a mixing time of 5 min was selected to achieve good mixing. Next, the extruded products were post-processed into dumbbell-shaped specimens via Haake Mini-jet micro piston injection moulding machine (Thermo Fisher Scientific, USA) to obtain the tensile test samples according to ISO 527-2-1BA standard. The cylinder temperature was set to 320 °C, while 110 °C was used for the mould. The injection moulding system was operated at 120 MPa (for 14 s) followed by the post pressure of 70 MPa (for 7 s), ensuring a complete filling of the mould. To improve the efficiency of the injection moulding process, the nanocomposite was heated for around 5 min before it was used in the moulding system.

2.3. Characterisation

Tensile tests on nanocomposites were carried out using an Instron 4301 universal tensile testing machine with a 5 kN load cell according to the ISO 527-2-1BA standards. All these tests were operated at a temperature of 23 °C (±2 °C) and relative humidity of 50 (±10%) under a tensile rate of 2 mm/min. Thermal stability tests of the nanocomposites were analysed using a thermogravimetric analyser (Q500, TA Instruments) with a scan range from 30 °C to 1100 °C at a constant heat rate of 10 °C/min and a continuous 50 mL/min of N_2 flow. DSC studies were conducted by a TA Q100 DSC instrument by heating the specimens from 35 °C to 300 °C under a constant heat rate of 10 °C/min. For the thermal tests, three samples (each weighing 2–20 mg and cut from the same position of every specimen) from each category (listed in Table 2) were used to increase the reliability and accuracy of data and then the average was taken for the analysis.

3. Results and discussion

3.1. Mass

As listed in Table 2, PC (both virgin and recycled) and GNP were formulated into 6 samples under 4 different processing conditions and the weight of the tensile test samples at each of these conditions was measured and reported in Fig. 1. Furthermore, the physical appearance of the fractured/tested tensile test samples is shown in Fig. 2. The weight of the virgin PC/GNP specimen gradually increased with increasing GNPs loading and showed positive growth with the processing speed. This could be because the higher shear force generated at higher processing speeds enables GNP to mix more thoroughly with PC. Moreover, the weight is also increasing with the process set temperature, which might be caused by the low viscosity of PC at higher temperatures enabling the mixture to pack properly, increasing the specific weight. The recycled PC shows a reduction in weight under 1 wt.-% of GNP loading, although the weight has increased for higher loadings from 2 wt.-% to 10 wt.-%. The reduction of weight at 1 wt.-% GNP loading can result from the escape of one or many ingredients due to the structural damage caused by the shear force during polymer processing.

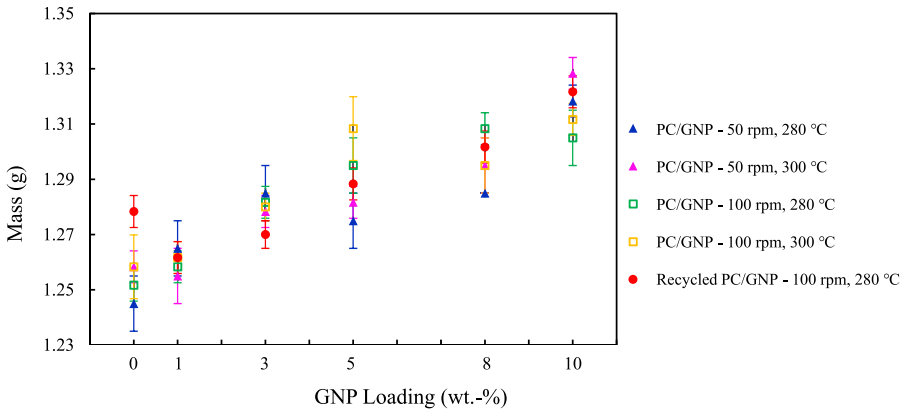

Fig. 1. PC/GNP and recycled PC/GNP nanocomposite mass vs GNP Loading under different process parameters.

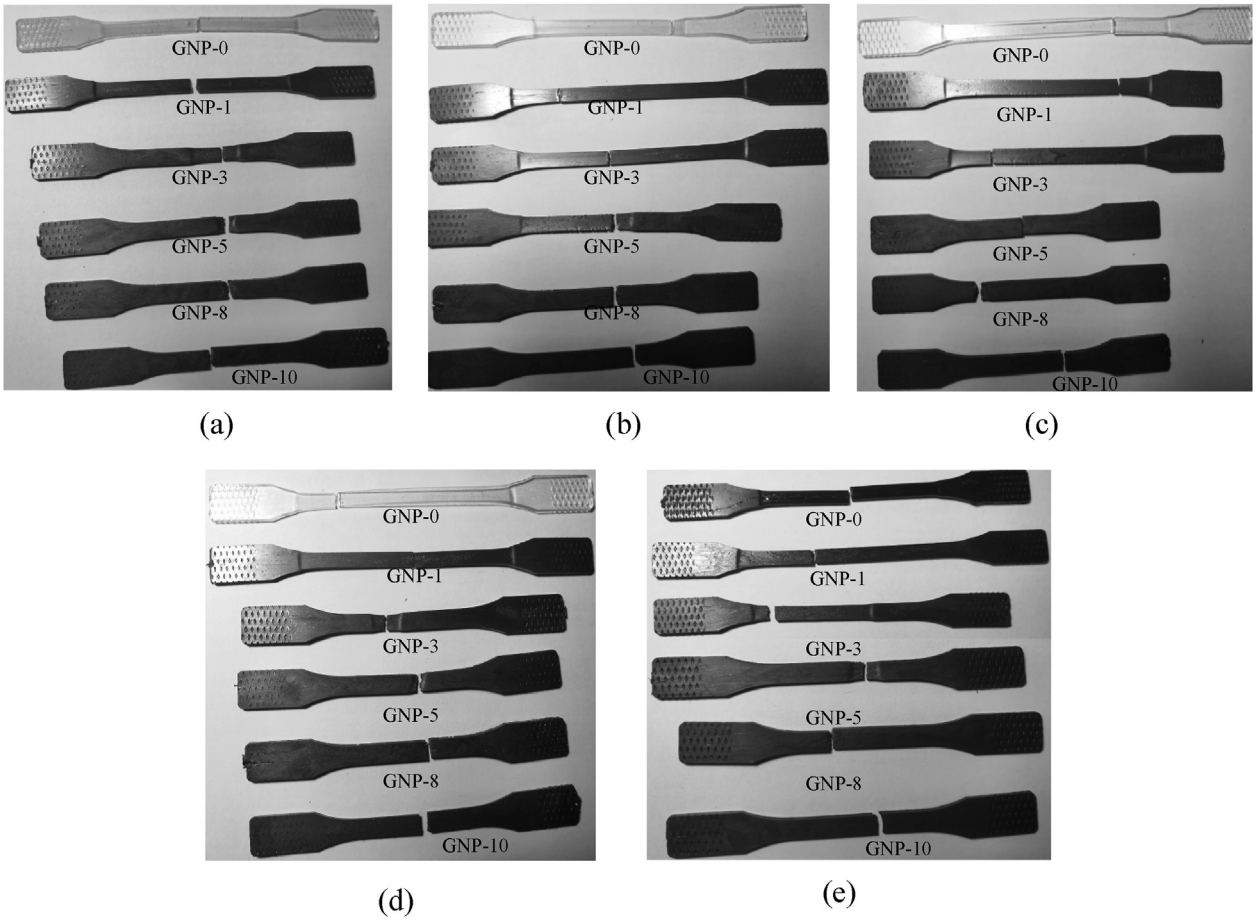

Fig. 2. The physical appearance of the fractured/tested nanocomposites processed under different conditions: (a) Virgin PC mixed with M15 GNP at 50 rpm and 280 °C; (b) Virgin PC mixed with M15 GNP at 100 rpm and 280 °C; (c) Virgin PC mixed with M15 GNP at 100 rpm and 300 °C; (d) Virgin PC mixed with M15 GNP at 50 rpm and 300 °C; (e) Recycled PC mixed with M15 GNP at 100 rpm and 280 °C.

3.2. Mechanical properties

The most frequently evaluated tensile properties (stress-strain relation, elastic modulus, tensile strength, and elongation to break) are presented in Figs. 3 and 4. According to the evaluated stress-strain relation of the nanocomposites (Fig. 3), a general trend of reduction in elongation to break and increment in the tensile stress is observable with the increasing GNP loading for all the processing conditions. Higher processing speed tends to increase the elongation to break, and the effect is more visible from the nanocomposites with low filler concentration. The largest change in elongation to break is observable in 3 wt.-% GNP loading, where the values change from 36.8% to 105.9% under 280 °C and from 32.2% to 98.8% under 300 °C. On the other hand, higher processing temperature has led to a slight reduction in the elongation to break, which is more noticeable in nanocomposites with high GNP

loading. Comparatively, recycled PC-based nanocomposites show similar but slightly lower elongation to break to the values shown by virgin PC-based nanocomposites under the same GNP loading. The effect of the processing speed, barrel/die set temperature, filler concentration and PC type on the tensile properties (this study) are extensively discussed in this section.

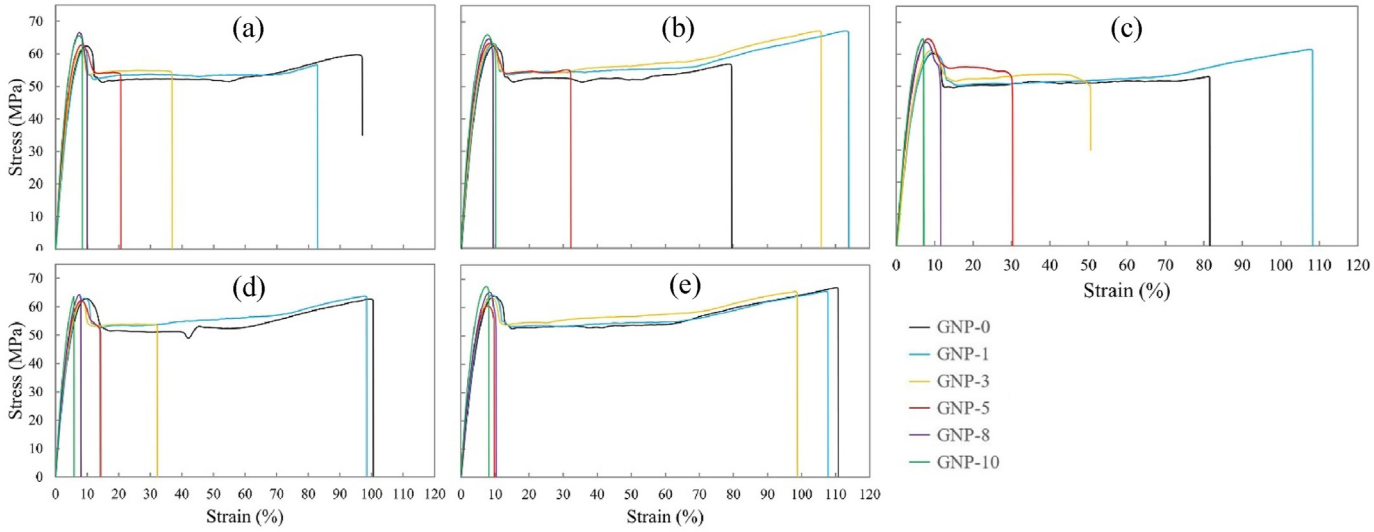

Fig. 3. Stress-strain curves of the composite material: (a) Virgin PC mixed with M15 GNP at 50 rpm and 280 °C; (b) Virgin PC mixed with M15 GNP at 100 rpm and 280 °C; (c) Recycled PC mixed with M15 GNP at 100 rpm and 280 °C; (d) Virgin PC mixed with M15 GNP at 50 rpm and 300 °C; (e) Virgin PC mixed with M15 GNP at 100 rpm and 300 °C.

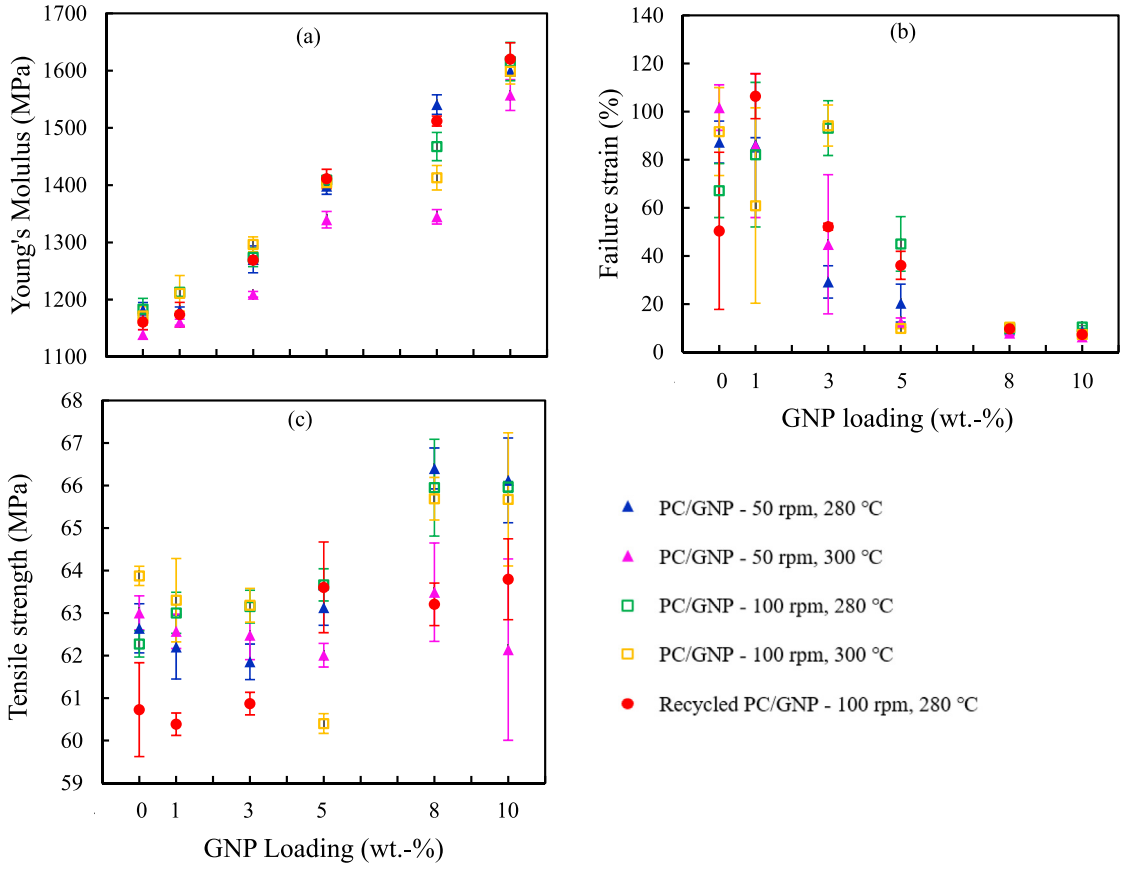

Fig. 4. (a) Young's modulus vs the GNPs Loading; (b) Yield strength against the GNPs Loading; (c) Failure strain against GNPs Loading with different process parameters of PC/GNP and recycled PC/GNP nanocomposite.

3.2.1. Effect of processing speed

Fig. 4 shows the variation of Young's modulus (Fig. 4a), failure strain (Fig. 4b) and tensile strength (Fig. 4c) for each processing condition of Virgin PC/GNP and 100 rpm/280 °C processed recycled PC/GNPs composites. A weak positive trend can be observed in Young's modulus with the processing speed, where Young's modulus has achieved a slight improvement in each sample under the same temperature. A deviation can be seen in GNP loading of 8 wt.-% at 280 °C, which might be resulted from uneven mixing during the processing stage [114] or agglomerate formation under higher loading of larger GNP particle size [36,64,115,116]. The yield strength indicates a mixed behaviour with the processing speed, where it has improved under higher speeds for the samples made at 300 °C (except GNP 5 wt.-%, which might be an error), while for the samples made at 280 °C, an increment is shown up to 5 wt.-% and a reduction for 8 and 10 wt.-% GNP loadings. As shown in Fig. 4c, higher processing speeds have enhanced the failure stain, where a significant improvement can be seen in the sample with 3 wt.-% GNP loading. Cho and Paul [88] have presented a similar type of behaviour in tensile properties with the processing speed on Nylon 6/organoclay nanocomposites. They have observed a slight increase in all three properties (under higher processing speeds) discussed above and concluded that this enhancement is due to the more significant hydrodynamic stresses induced by the shear rates during higher speeds. Under significantly low hydrodynamic stresses, the interfacial forces become dominant and tend to increase the number of agglomerates within the nanocomposite [116]. Thus, the property enhancement in higher processing speed can be explained due to the low agglomeration under more significant hydrodynamic stresses induced.

3.2.2. Barrel/die set temperature

As shown in Fig. 4a, a reduction in Young's modulus can be noticed at the higher barrel/die set temperature under both processing speeds. Higher yield strength (Fig. 4c) can be observed at the higher temperature in the low filler concentration (1–5 wt.-% GNP) region, while the trend changes and gives lower yield strength values at GNP loading of 8 and 10 wt.-%. When considering the failure strain (Fig. 4b), it gets reduced with rising temperature. This weakening effect is much visible in the samples processed at 100 rpm, where a maximum reduction of 72% is given under 5 wt.-% GNP loading. The temperature-dependent behaviour of the tensile properties has also been reported in some previous studies [117–119]. Lin et al. [117], in their molecular dynamics simulations of graphene/PMMA nanocomposite system, have observed a decrease in Young's modulus as the temperature rises from 300 K to 500 K. Moreover, they have reported that Young's modulus of the nanocomposites with higher graphene volume fraction are more sensitive to the temperature and show more significant reductions of modulus with rising temperature. This behaviour is also observable in our results (Fig. 4a), where the difference of Young's modulus between two temperatures is increasing (for both processing speeds) with GNP loading up to 8 wt.-%. Sun et al. [118] also reported similar findings for Young's modulus in their atomistic study on the mechanical behaviours of polymer nanocomposite reinforced with defective graphene using molecular dynamics simulations. They [118] conclude this behaviour is due to the gain of sufficient energy by nanocomposite atoms to overcome the activation energy barrier and become much more active, thus deteriorating the deformation resistance and Young's modulus of the nanocomposite. The variations of the mechanical properties with temperature reported in our study are consistent with the temperature-dependent properties of the single-layer graphene sheets [120], where Young's modulus and Ultimate strength are reported to decrease with increasing temperature. Further, the results agree with the multilayer graphene sheets [121], which have shown a continuous reduction in Young's modulus, Fracture stress and fracture strain with increasing temperature.

3.2.3. Filler concentration

According to this study's results, adding GNP to the PC matrix has altered the tensile properties of both virgin and recycled PC matrix composites. The yield point has shifted to higher stress and lower strain under increasing GNP loading (Fig. 3), which may be occurred due to the mobility restriction of polymer chains as a result of the large aspect ratio of GNP and its interaction with the PC matrix [8,14,55]. The Young's modulus shows (Fig. 4-a) superliner increases with the filler concentration, where the maximum enhancement of ~33% of the modulus is given for the PC/GNP composites with 10 wt.-% GNP. This superliner relation indicates an additional enhancement at higher GNP loadings, which has also been reported in previous studies [14,122–125]. This phenomenon, where the rate of the increase of modulus increases with increasing filler concentration, was studied by Guth and Gold [126] and defined as accelerated stiffening. Many theories, such as Guth and Gold [126], Jamming theory [122], and shear-lag/rule-of-mixtures theory [14], have been employed to describe the accelerated stiffening up to a certain extent.

On the other hand, the yield strength displays uneven variations with increasing filler content, and the trends are observable in Fig. 4c. A decreasing trend of strength can be seen at low GNP loadings (except for samples processed under 100 rpm at 280 °C), while a clear development is visible between 5 and 8 wt.-% GNP loadings. Moreover, the 10 wt.-% GNP loading gives slightly reduced strength values compared to 8 wt.-% loading except for the sample processed under 50 rpm and 300 °C, where a steep decrease is observable. Shen et al. [41] have reported a similar downward movement under a low GNP loading (until 1.5 wt.-%) in their study of GNP/Epoxy composites. Moreover, they have concluded that this downtrend can be attributed to the effects such as nonuniform dispersion of nanofillers and/or the presence of voids within the composites structure [41]. The enhancement of tensile strength at 8 wt.-% GNP might occur due to the good distribution and interfacial adhesion between PC matrix and fillers, enabling a better load transfer from matrix to fillers [54,127]. Then, the reduction in yield strength from 8 wt.-% to 10 wt.-% samples can be attributed to increasing in voids in composites under higher nanoparticle contents [128,129] and agglomerate formation under higher loading of larger GNP particle size [36,64,115,116]. In contrast to the findings present in this paper, Lago et al. [73] have reported an increase in strength after adding 0.5 wt.-% of graphene to PC and a saturation-like behaviour with increasing graphene loadings (up to 3 wt.-%). This contradictory result could be associated with the different processing methods (solution blending in Lago et al. and melt mixing in our study) and properties of graphene used (natural graphite flakes (+100 mesh (≥75% min)) used in Lago et al. and M15 GNP in our study). However, further studies to determine this phenomenon are needed.

The failure strain decreases exponentially with the increase of filler loading. Composites with low GNP loadings show ductile behaviour, while high filler concentrations display brittle behaviour. This transitional behaviour is reasonably visible in Figs. 3 and 4(b), where higher failure stains can be seen for 0, 1 and 3 wt.-% GNP and relatively small failure stains for other filler concentrations. This ductile to brittle transition has also been observed by Chieng et al. [40] in their study on GNP-reinforced poly(lactic acid)/poly(ethylene glycol) nanocomposites processed *via* a melt blending method. The decrease of failure strain with increasing GNP concentration is commonly observable in graphene-based polymer nanocomposites [14,40,55,130]. The formation of agglomerates may cause this reduction at higher GNP content [54,115,131] due to the high level of

GNP concentration where the failure was introduced during elongation as an outcome of stress concentration [130].

3.2.4. Type of polymer

As mentioned above, the processing of recycled PC is a new area; hence, previous research is seldom. Therefore, one of the objectives of this study is to investigate the properties of GNP-reinforced recycled PC nanocomposites. In order to achieve this objective, recycled PC and its nanocomposites were processed at 100 rpm and 280 °C, then tested and compared with the virgin PC/GNP composites made under the same processing conditions. As evident from Fig. 1, the mass of the recycled PC is greater than the virgin PC, which might be due to the presence of additional substances in the recycled PC. This claim is also visible in Fig. 2, where the colours of recycled PC samples (0 wt.-% GNP) and virgin PC samples (0 wt.-% GNP) are notably different. In regard to the mechanical properties, recycled PC exhibits lower Young's modulus, yield strength and failure strain than the virgin PC, which might not be surprising. However, the level of enhancement of the mechanical properties with increasing filler content is superior in recycled PC/GNP composites. Young's modulus and failure stain of recycled PC/GNP composites depict similar trends with rising GNP loading as virgin PC-based composites. The yield strength of recycled PC-based composites shows a nonlinear positive relationship with the increasing filler content. This trend is significantly different from the trend displayed by virgin PC-based composites; thus, further studies must be conducted to understand this phenomenon.

3.3. Thermal properties

3.3.1. Thermal stability

The thermal behaviour of the PC/GNP and recycled PC/GNP composites are discussed in terms of thermal stability and glass transition temperature. Fig. 5 depicts the TGA and DTG thermograms of Virgin PC and PC/GNP composites with 1, 3, 5, 8 and 10 wt.-% of GNP loading. The pyrolysis of virgin PC, which is due to the separation of carbonate groups [132], starts (5% weight loss was considered) at ~ 470 °C, whereas the 5% weight loss of all the composites occurred at slightly higher temperatures than 470 °C, indicating that the presence of GNP improves the thermal stability of PC. This enhancement of thermal stability might cause by the mobility reduction of polymer chains imposed by the fillers [55]. The highest thermal stability indicates in the composite loaded with 1 wt.-% GNP. The maximum degradation temperature of 1 wt.-% GNP composite that was evaluated at the peak of the DTG curve is 523.61 °C and is a 13.95 °C rise compared to the maximum degradation temperature of virgin PC. A study by Lago et al. [73] has also reported an 86 °C increment in maximum degradation temperature with 1 wt.-% GNP content in virgin PC-based nanocomposite. In their study, graphene-based PC composites have been prepared by a solution bending method, which is reported to provide better mixing than the melt blending methods [78,79].

After 1 wt.-% GNP loading, the thermal stability of the composites displays a gradual decrease with the increasing GNPs content. This can be clearly seen from the evaluated maximum degradation temperatures from DTG curves, which are recorded in Table 3.

The TGA and DTG results of recycled PC and its nanocomposites with 1, 3, 5, 8 and 10 wt.-% of GNP loading are shown in Fig. 6. The main weight loss (5 wt.-%) of recycled PC starts at ~455 °C, indicating the lowest thermal stability among the recycled PC/GNP composites. The degradation temperature of recycled PC is evaluated as 497.49 °C. As opposed to the behaviour shown by virgin PC/GNP composites, the recycled PC/GNP composites display a slight growth in degradation temperature; thereby, the thermal stability increases with GNP loading. The evaluated temperature of samples with 1, 3, 5, 8 and 10 wt.-% GNP is shown in Table 3. As reported in the literature, recycled PC may contain different percentages of

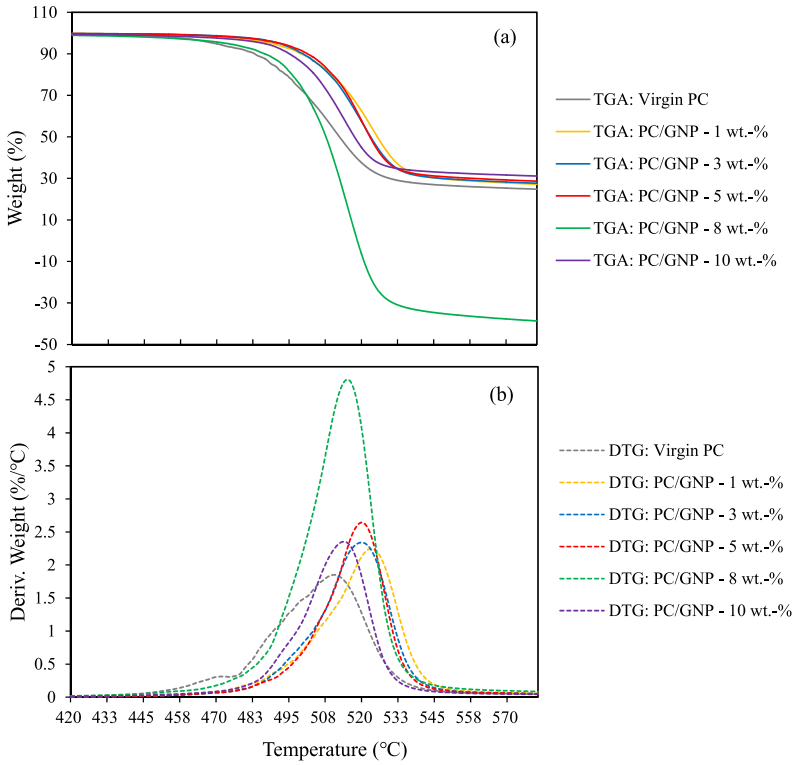

Fig. 5. Partial (a) TGA and (b) DTG curves (420–580 °C) of virgin PC and PC/GNP composites. All the samples were made under 100 rpm and 280 °C processing conditions.

Table 3
Maximum degradation temperature of virgin PC-based and recycled PC-based nanocomposites. All the samples are made under 100 rpm and 280 °C processing conditions.

GNP content/wt.-%	Maximum degradation temperature/°C	
	Virgin PC/GNP composite	Recycled PC/GNP composite
0	509.66	497.49
1	523.61	507.03
3	521.09	508.31
5	520.28	508.66
8	515.56	509.45
10	513.66	509.55

impurities [106,133,134] and the purity level and the nature of the impurities can significantly affect the properties [106,134]. The difference in the purity level of the recycled PC (which alters the thermal properties of recycled PC) with the virgin PC could explain the above-discussed discrepancy in thermal stability behaviour between the two nanocomposites.

3.3.2. Glass transition temperature

The glass transition temperature is significant to understanding the performance and behaviour of a polymer. This study used DSC testing to evaluate the glass transition temperature (T_g) of the GNP-reinforced virgin PC-based and recycled PC-based nanocomposites made under 100 rpm and 280 °C processing conditions. For the DSC analysis, the temperature is increased by 10 °C/min from 35 to 300 °C. The thermogram of each composite is displayed in Fig. 7, and the evaluated transition temperatures are reported in Table 4. The evaluated T_g of virgin PC from this study agrees with the values reported in the literature [135]. However, in Fig. 7a, a heat peak is observable around T_g, which is an irregular behaviour for an amorphous polymer such as PC. This phenomenon could be resulted from (i) partly crystalline PC in the composite or (ii) energy added to the composite via GNP reinforcement or due to the combination of both (i) and (ii). This irregular behaviour is less depicted in recycled PC, where an insignificant heat peak can be seen in DSC analysis. This might be due to the presence of other substances in recycled PC and their interaction with GNP after intercalation.

The evaluated T_g values (correspond to the midpoint of the glass transition region) presented in Table 4 depict that the effect of GNP on T_g is incidental for both virgin and recycled PC composites. The T_g of virgin PC shows a slight increase with 1 wt.-% GNP loading but starts to decrease with increasing GNP content. The lowest T_g of virgin PC-based composites exhibit in 8 wt.-% GNP and is lower than that of virgin PC. On the other hand, recycled PC shows a close but relatively higher transition temperature than virgin PC. This difference in T_g is another evidence supporting the claim of the presence of other substances in recycled PC. The observed variation of T_g in the current study with increasing GNP content in recycled PC-based composites is obscure and thus has to be tested further with a higher number of specimens covering a wide operating and processing range. For recycled PC composites, first, T_g reduces with 1 wt.-% GNP and increase under 3 wt.-% loading. Then a gradual drop can be seen until 8 wt.-%, where a modest increment is shown with 10 wt.-% GNP loading.

The glass transition, which occurs due to freezing the motion of polymer chain segments [136], can be studied through free volume and polymer chain mobility. Several past studies which had examined the glass transition behaviour of graphene-based nanocomposites have reported an increase in T_g after the addition of graphene and a gradual decrease afterwards with increasing graphene content [58,137–141]. The study by Ramanathan et al. [58] has explained a similar behaviour (reduction in T_g with rising filler loading) using the observation of the interparticle distances of graphene/PMMA nanocomposites. They have observed a decrease in interparticle spacing with increasing filler (as received graphite

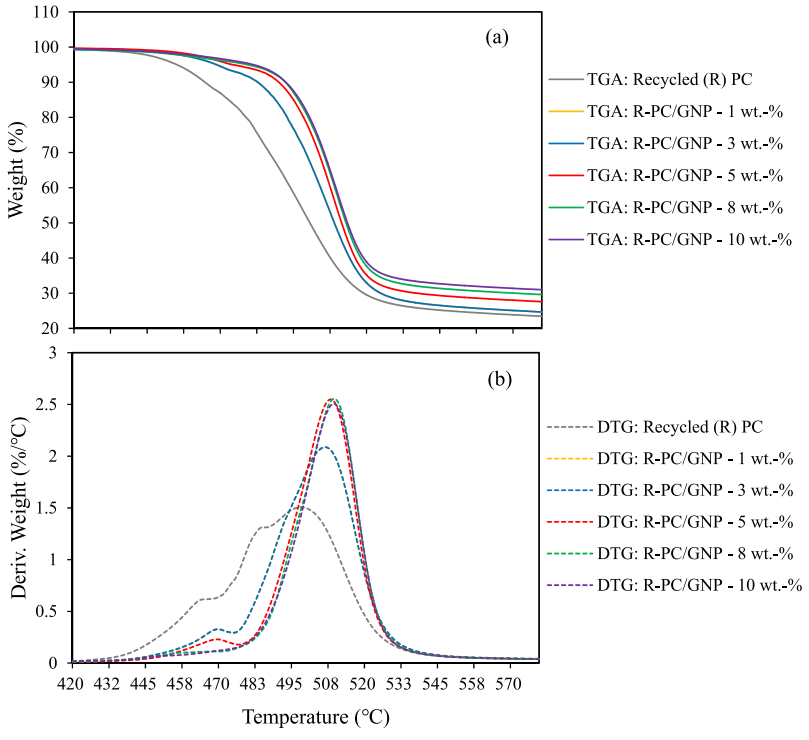

Fig. 6. Partial (a) TGA and (b) DTG curves (420–580 °C) of recycled PC and recycled PC/GNP composites. All the samples are made under 100 rpm and 280 °C processing conditions.

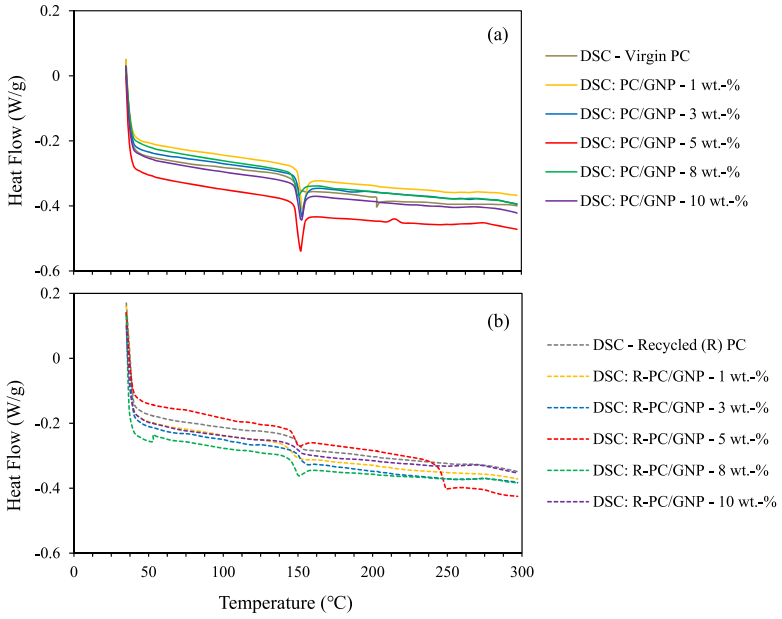

Fig. 7. DSC thermograms of (a) virgin PC and PC/GNPs composites; (b) recycled PC and recycled PC/GNPs composites. All the samples are made under 100 rpm and 280 °C processing conditions.

and exfoliated graphite) loading and suggest this decrease promotes local particle clustering, causing an increase in particle-particle interaction and thus a decrease in the opportunity for strong particle–polymer bonding which leads to the reduction in T_g. Sheng et al. [141], in their molecular dynamic simulations on polyethylene/graphene nanocomposites, emphasise that the reduction in T_g observed in their findings is because the graphene act as a plasticising agent which enhances the polymer chain motion resulting in reduced T_g. Moreover, they suggest that the effect of plasticiser may depend on the graphene content, which describes the gradual reduction of T_g with increasing filler loading.

Further explanation of this decrease in T_g can be taken considering the decrease of the free volume in the composite [142]. The polymeric free volume model by White and Lipson [142] describes the temperature-dependent nature of the free volume and shows a positive relationship between the free volume and the experimentally measured glass transition temperature. The increase in GNP content leads to a decrease in free volume; hence, the reduction in T_g can also be associated with the reduction in free volume (according to the model proposed by White and Lipson [142]). Therefore, one can assume that the gradual decrease in T_g notably observed with PC/GNP nanocomposites in our study is due to one or a combination of the above-mentioned available explanations. Recycled PC/GNP nanocomposites display a similar decrease in T_g with filler loading, which can be reasonably explained in terms of the reduction of the free volume. However, these assumptions need to be further analysed and tested with a higher number of samples to widen the understanding.

Table 4
Glass transition temperatures of virgin PC, virgin PC/GNP composites, recycled PC, and recycled PC/GNP composites. All the samples are made under 100 rpm and 280 °C processing conditions.

GNP content (wt.-%)	Glass transition temperature (T_g)/°C	
	Matrix material: Virgin PC	Matrix material: Recycled PC
0	148.73	149.70
1	152.38	144.98
3	151.74	151.34
5	150.28	147.90
8	148.84	147.33
10	150.71	150.22

4. Conclusions

This research aimed to investigate the mechanical and thermal properties of GNP-reinforced virgin and recycled PC nanocomposites. The nanocomposites were successfully processed using a twin screw extruder at various processing parameters, and the results were examined considering various key processing parameters such as filler concentration, processing speed, barrel/die set temperature, and PC type. The mechanical properties were investigated by tensile test, while DSC and TGA testing characterised the thermal properties. Tensile test results showed that Young's modulus of the nanocomposites is superior to the matrix material (with no GNP), where the maximum improvement of Young's modulus was evaluated as ~33% and ~39.5% for GNP loading of 10 wt.-% for virgin PC/GNP and recycled PC/GNP, respectively. The failure strain of both virgin PC-based and recycled PC-based composites decreased exponentially, and a ductile to brittle transition was also observed with rising filler loading. From the considered key processing parameters, processing speed and barrel/die set temperature displayed only a slight influence on the mechanical properties, while the filler concentration was identified as the most influential parameter. On the other hand, the thermal properties of the nanocomposites showed insignificant variation with the matrix material (with no GNP), indicating that the GNP hardly affects the thermal stability and glass transition temperature of the virgin or recycled PC. Recycled PC showed lower mechanical and thermal properties than virgin PC but exhibited better enhancement trends when mixed with GNP. Therefore, further studies such as morphology analysis and stress transfer efficiency are needed to develop a better understanding of recycled PC/GNP composites and their potential in industrial applications. Such knowledge would help to improve the use of recycled materials, promoting a sustainable and circular economy.

Conflicts of interest

The authors declare that there is no conflicts of interest.

Abbreviations

T_g	Glass transition temperature
2D	Two dimensional
DSC	Differential scanning calorimetry
DTG	Derivative thermogravimetric
GNP	Graphene nano-platelets
HDPE	High-density polyethylene
PC	Polycarbonate
PMMA	Poly(methyl methacrylate)
TGA	Thermogravimetric analysis
TRG	Thermally reduced graphene

References

[1] B.T. Åström, Manufacturing of Polymer Composites, Routledge, 2018, https://doi.org/10.1201/9780203748169.

[2] C. Abeykoon, A.L. Kelly, J. Vera-Sorroche, E.C. Brown, P.D. Coates, J. Deng, K. Li, E. Harkin-Jones, M. Price, Process efficiency in polymer extrusion: correlation between the energy demand and melt thermal stability, Appl. Energy 135 (2014) 560–571, https://doi.org/10.1016/j.apenergy.2014.08.086.

[3] K.U.A.K.Y.K.T.K.O., A. Okada, Synthesis and properties of nylon-6/clay hybrids, in: D.W. Schaefer, J.E. Mark (Eds.), Polymer Based Molecular Composites vol. 171, MRS Symposium Proceedings, Materials Research Society, Pittsburgh PA, 1990, pp. 45–50.

[4] R.F. Landel, L.E. Nielsen, Mechanical Properties of Polymers and Composites, CRC Press, 1993.

[5] J. Zhu, C. Abeykoon, N. Karim, Investigation into the effects of fillers in polymer processing, International Journal of Lightweight Materials and Manufacture 4 (2021) 370–382, https://doi.org/10.1016/j.ijlmm.2021.04.003.

[6] R. v Kurahatti, A.O. Surendranathan, S.A. Kori, N. Singh, A. v Ramesh Kumar, S. Srivastava, Defence Applications of Polymer Nanocomposites, DESIDOC, 2010.

[7] G. Mittal, V. Dhand, K.Y. Rhee, S.J. Park, W.R. Lee, A review on carbon nanotubes and graphene as fillers in reinforced polymer nanocomposites, J. Ind. Eng. Chem. 21 (2015) 11–25, https://doi.org/10.1016/j.jiec.2014.03.022.

[8] J.H. Lee, J. Marroquin, K.Y. Rhee, S.J. Park, D. Hui, Cryomilling application of graphene to improve material properties of graphene/chitosan nanocomposites, Compos. B Eng. 45 (2013) 682–687, https://doi.org/10.1016/j.compositesb.2012.05.011.

[9] R.A. Hule, D.J. Pochan, Polymer nanocomposites for biomedical applications, MRS Bull. 32 (2007) 354–358, https://doi.org/10.1557/mrs2007.235.

[10] L. Zhang, C. Shi, K.Y. Rhee, N. Zhao, Properties of Co 0.5Ni 0.5Fe 2O 4/carbon nanotubes/polyimide nanocomposites for microwave absorption, Compos. A: Appl. Sci. Manuf. 43 (2012) 2241–2248, https://doi.org/10.1016/j.compositesa.2012.08.014.

[11] S.H. Liao, C.Y. Yen, C.C. Weng, Y.F. Lin, C.C.M. Ma, C.H. Yang, M.C. Tsai, M.Y. Yen, M.C. Hsiao, S.J. Lee, X.F. Xie, Y.H. Hsiao, Preparation and properties of carbon nanotube/polypropylene nanocomposite bipolar plates for polymer electrolyte membrane fuel cells, J. Power Sources 185 (2008) 1225–1232, https://doi.org/10.1016/j.jpowsour.2008.06.097.

[12] D.Y. Godovsky, Device applications of polymer-nanocomposites, 2000, pp. 163–205, https://doi.org/10.1007/3-540-46414-X_4.

[13] Reportlinker.com, Global polymer fillers industry. Https://Www.Reportlinker.Com/P05900112/?Utm_source=GNW, 2020.

[14] M. Liu, I.A. Kinloch, R.J. Young, D.G. Papageorgiou, Modelling mechanical percolation in graphene-reinforced elastomer nanocomposites, Compos. B: Eng. 178 (2019), https://doi.org/10.1016/j.compositesb.2019.107506.

[15] E.T. Thostenson, Z. Ren, T.-W. Chou, Advances in the science and technology of carbon nanotubes and their composites: a review, n.d. www.elsevier.com/locate/compscitech.

[16] D. Cai, K. Yusoh, M. Song, The mechanical properties and morphology of a graphite oxide nanoplatelet/polyurethane composite, Nanotechnology 20 (2009), https://doi.org/10.1088/0957-4484/20/8/085712.

[17] B.A. Higgins, W.J. Brittain, Polycarbonate carbon nanofiber composites, Eur. Polym. J. 41 (2005) 889–893, https://doi.org/10.1016/j.eurpolymj.2004.11.040.

[18] Y. Geng, M.Y. Liu, J. Li, X.M. Shi, J.K. Kim, Effects of surfactant treatment on mechanical and electrical properties of CNT/epoxy nanocomposites, Compos. A: Appl. Sci. Manuf. 39 (2008) 1876–1883, https://doi.org/10.1016/j.compositesa.2008.09.009.

[19] K.S. Novoselov, A.K. Geim, S.v. Morozov, D. Jiang, Y. Zhang, S.v. Dubonos, I.v. Grigorieva, A.A. Firsov, Electric field in atomically thin carbon films, Science 306 (2004) 666–669, https://doi.org/10.1126/science.1102896.

[20] X. Huang, X. Qi, F. Boey, H. Zhang, Graphene-based composites, Chem. Soc. Rev. 41 (2012) 666–686, https://doi.org/10.1039/C1CS15078B.

[21] M.H. Islam, M.R. Islam, M. Dulal, S. Afroj, N. Karim, The effect of surface treatments and graphene-based modifications on mechanical properties of natural jute fiber composites: a review, iScience 25 (2022) 103597, https://doi.org/10.1016/j.isci.2021.103597.

[22] N. Karim, F. Sarker, S. Afroj, M. Zhang, P. Potluri, K.S. Novoselov, Sustainable and multifunctional composites of graphene-based natural jute fibers, Adv. Sustainable Syst. 5 (2021) 2000228, https://doi.org/10.1002/adsu.202000228.

[23] J. Abraham, K.S. Vasu, C.D. Williams, K. Gopinadhan, Y. Su, C.T. Cherian, J. Dix, E. Prestat, S.J. Haigh, I.v. Grigorieva, P. Carbone, A.K. Geim, R.R. Nair, Tunable sieving of ions using graphene oxide membranes, Nat. Nanotechnol. 12 (2017) 546–550, https://doi.org/10.1038/nnano.2017.21.

[24] N. Karim, S. Afroj, D. Leech, A.M. Abdelkader, Flexible and wearable graphene-based <scp>E</scp> -textiles, in: Oxide Electronics, Wiley, 2021, pp. 21–49, https://doi.org/10.1002/9781119529538.ch2.

[25] G. Hu, J. Kang, L.W.T. Ng, X. Zhu, R.C.T. Howe, C.G. Jones, M.C. Hersam, T. Hasan, Functional inks and printing of two-dimensional materials, Chem. Soc. Rev. 47 (2018) 3265–3300, https://doi.org/10.1039/C8CS00084K.

[26] O. Ogbeide, G. Bae, W. Yu, E. Morrin, Y. Song, W. Song, Y. Li, B. Su, K. An, T. Hasan, Inkjet-Printed rGO/binary metal oxide sensor for predictive gas sensing in a mixed environment, Adv. Funct. Mater. (2022) 2113348, https://doi.org/10.1002/adfm.202113348.

[27] M.R. Islam, S. Afroj, C. Beach, M.H. Islam, C. Parraman, A. Abdelkader, A.J. Casson, K.S. Novoselov, N. Karim, Fully printed and multifunctional graphene-based wearable e-textiles for personalised healthcare applications, iScience 25 (2022) 103945, https://doi.org/10.1016/j.isci.2022.103945.

[28] Y. Yang, A.M. Asiri, Z. Tang, D. Du, Y. Lin, Graphene based materials for biomedical applications, Mater. Today 16 (2013) 365–373, https://doi.org/10.1016/j.mattod.2013.09.004.

[29] A.M. Abdelkader, Electrochemical synthesis of highly corrugated graphene sheets for high performance supercapacitors, J. Mater. Chem. 3 (2015) 8519–8525, https://doi.org/10.1039/C5TA00545K.

[30] M.D. Stoller, S. Park, Z. Yanwu, J. An, R.S. Ruoff, Graphene-Based ultracapacitors, Nano Lett. 8 (2008) 3498–3502, https://doi.org/10.1021/nl802558y.

[31] C. Lee, X. Wei, J.W. Kysar, J. Hone, Measurement of the elastic properties and intrinsic strength of monolayer graphene, Science 321 (2008) (1979) 385–388, https://doi.org/10.1126/science.1157996.

[32] A.A. Balandin, S. Ghosh, W. Bao, I. Calizo, D. Teweldebrhan, F. Miao, C.N. Lau, Superior thermal conductivity of single-layer graphene, Nano Lett. 8 (2008) 902–907, https://doi.org/10.1021/nl0731872.

[33] K.S. Novoselov, A.K. Geim, S.v. Morozov, D. Jiang, M.I. Katsnelson, I.v. Grigorieva, S.v. Dubonos, A.A. Firsov, Two-dimensional gas of massless Dirac fermions in graphene, Nature 438 (2005) 197–200, https://doi.org/10.1038/nature04233.

[34] R. Sengupta, M. Bhattacharya, S. Bandyopadhyay, A.K. Bhowmick, A review on the mechanical and electrical properties of graphite and modified graphite reinforced polymer composites, Prog. Polym. Sci. 36 (2011) 638–670, https://doi.org/10.1016/j.progpolymsci.2010.11.003.

[35] V.C. Tung, M.J. Allen, Y. Yang, R.B. Kaner, High-throughput solution processing of large-scale graphene, Nat. Nanotechnol. 4 (2009) 25–29, https://doi.org/10.1038/nnano.2008.329.

[36] B. Li, W.H. Zhong, Review on polymer/graphite nanoplatelet nanocomposites, J. Mater. Sci. 46 (2011) 5595–5614, https://doi.org/10.1007/s10853-011-5572-y.

[37] L.M. Viculis, J.J. Mack, O.M. Mayer, H.T. Hahn, R.B. Kaner, Intercalation and exfoliation routes to graphite nanoplatelets, J. Mater. Chem. 15 (2005) 974–978, https://doi.org/10.1039/b413029d.

[38] W. Guoxiu, Y. Juan, P. Jinsoo, G. Xinglong, W. Bei, L. Hao, Y. Jane, Facile synthesis and characterisation of graphene nanosheets, J. Phys. Chem. C 112 (2008) 8192–8195, https://doi.org/10.1021/jp710931h.

[39] G. Wang, X. Shen, B. Wang, J. Yao, J. Park, Synthesis and characterisation of hydrophilic and organophilic graphene nanosheets, Carbon N Y 47 (2009) 1359–1364, https://doi.org/10.1016/j.carbon.2009.01.027.

[40] B.W. Chieng, N.A. Ibrahim, W.M.Z.W. Yunus, M.Z. Hussein, Poly(lactic acid)/poly(ethylene glycol) polymer nanocomposites: effects of graphene nanoplatelets, Polymers 6 (2014) 93–104, https://doi.org/10.3390/polym6010093.

[41] M.Y. Shen, T.Y. Chang, T.H. Hsieh, Y.L. Li, C.L. Chiang, H. Yang, M.C. Yip, Mechanical properties and tensile fatigue of graphene nanoplatelets reinforced polymer nanocomposites, J. Nanomater. 2013 (2013), https://doi.org/10.1155/2013/565401.

[42] T. Kuilla, S. Bhadra, D. Yao, N.H. Kim, S. Bose, J.H. Lee, Recent advances in graphene based polymer composites, Prog. Polym. Sci. 35 (2010) 1350–1375, https://doi.org/10.1016/j.progpolymsci.2010.07.005.

[43] V. Singh, D. Joung, L. Zhai, S. Das, S.I. Khondaker, S. Seal, Graphene based materials: past, present and future, Prog. Mater. Sci. 56 (2011) 1178–1271, https://doi.org/10.1016/j.pmatsci.2011.03.003.

[44] J.R. Potts, D.R. Dreyer, C.W. Bielawski, R.S. Ruoff, Graphene-based polymer nanocomposites, Polymer 52 (2011) 5–25, https://doi.org/10.1016/j.polymer.2010.11.042.

[45] H. Kim, A.A. Abdala, C.W. Macosko, Graphene/polymer nanocomposites, Macromolecules 43 (2010) 6515–6530, https://doi.org/10.1021/ma100572e.

[46] P. Cataldi, I.S. Bayer, G. Nanni, A. Athanassiou, F. Bonaccorso, V. Pellegrini, A.E. del Rio Castillo, F. Ricciardella, S. Artyukhin, M.-A. Tronche, Y. Gogotsi,

R. Cingolani, Effect of graphene nanoplatelet morphology on the elastic modulus of soft and hard biopolymers, Carbon N Y 109 (2016) 331–339, https://doi.org/10.1016/j.carbon.2016.08.026.
[47] A. Stonehouse, C. Abeykoon, Thermal properties of phase change materials reinforced with multi-dimensional carbon nanomaterials, Int. J. Heat Mass Transfer 183 (2022) 122166, https://doi.org/10.1016/j.ijheatmasstransfer.2021.122166.
[48] J. Parameswaranpillai, M.R. Sanjay, S.A. Varghese, S. Siengchin, S. Jose, N. Salim, N. Hameed, A. Magueresse, Toughened PS/LDPE/SEBS/xGnP ternary composites: morphology, mechanical and viscoelastic properties, Int. J. Lightweight Mater. Manuf. 2 (2019) 64–71, https://doi.org/10.1016/j.ijlmm.2018.12.003.
[49] A. Bianco, H.-M. Cheng, T. Enoki, Y. Gogotsi, R.H. Hurt, N. Koratkar, T. Kyotani, M. Monthioux, C.R. Park, J.M.D. Tascon, J. Zhang, All in the graphene family – a recommended nomenclature for two-dimensional carbon materials, Carbon N Y 65 (2013) 1–6, https://doi.org/10.1016/j.carbon.2013.08.038.
[50] G. Chen, W. Weng, D. Wu, C. Wu, J. Lu, P. Wang, X. Chen, Preparation and characterisation of graphite nanosheets from ultrasonic powdering technique, Carbon N Y 42 (2004) 753–759, https://doi.org/10.1016/j.carbon.2003.12.074.
[51] B. Shen, D. Lu, W. Zhai, W. Zheng, Synthesis of graphene by low-temperature exfoliation and reduction of graphite oxide under ambient atmosphere, J. Mater. Chem. C 1 (2013) 50–53, https://doi.org/10.1039/c2tc00044j.
[52] Y.-X. Pan, Z.-Z. Yu, Y.-C. Ou, G.-H. Hu, A New Process of Fabricating Electrically Conducting Nylon 6/Graphite Nanocomposites via Intercalation Polymerisation, 2000.
[53] J. Liang, Y. Xu, Y. Huang, L. Zhang, Y. Wang, Y. Ma, F. Li, T. Guo, Y. Chen, Infrared-triggered actuators from graphene-based nanocomposites, J. Phys. Chem. C 113 (2009) 9921–9927, https://doi.org/10.1021/jp901284d.
[54] L. Wang, J. Hong, G. Chen, Comparison study of graphite nanosheets and carbon black as fillers for high density polyethylene, Polym. Eng. Sci. 50 (2010) 2176–2181, https://doi.org/10.1002/pen.21751.
[55] X. Zhao, Q. Zhang, D. Chen, P. Lu, Enhanced mechanical properties of graphene-based polyvinyl alcohol composites, Macromolecules 43 (2010) 2357–2363, https://doi.org/10.1021/ma902862u.
[56] F. Sarker, P. Potluri, S. Afroj, V. Koncherry, K.S. Novoselov, N. Karim, Ultrahigh performance of nanoengineered graphene-based natural jute fiber composites, ACS Appl. Mater. Interfaces 11 (2019) 21166–21176, https://doi.org/10.1021/acsami.9b04696.
[57] F. Sarker, N. Karim, S. Afroj, V. Koncherry, K.S. Novoselov, P. Potluri, High-performance graphene-based natural fiber composites, ACS Appl. Mater. Interfaces 10 (2018) 34502–34512, https://doi.org/10.1021/acsami.8b13018.
[58] T. Ramanathan, S. Stankovich, D.A. Dikin, H. Liu, H. Shen, S.T. Nguyen, L.C. Brinson, Graphitic nanofillers in PMMA nanocomposites - an investigation of particle size and dispersion and their influence on nanocomposite properties, J. Polym. Sci., Part B: Polym. Phys. 45 (2007) 2097–2112, https://doi.org/10.1002/polb.21187.
[59] A. Yasmin, J.J. Luo, I.M. Daniel, Processing of expanded graphite reinforced polymer nanocomposites, Compos. Sci. Technol. 66 (2006) 1182–1189, https://doi.org/10.1016/j.compscitech.2005.10.014.
[60] S. Gupta, P. Raju Mantena, A. Al-Ostaz, Dynamic mechanical and impact property correlation of nanoclay and graphite platelet reinforced vinyl ester nanocomposites, J. Reinforc. Plast. Compos. 29 (2010) 2037–2047, https://doi.org/10.1177/0731684409341762.
[61] S. Ghose, D.C. Working, J.W. Connell, J.G. Smith, K.A. Watson, D.M. Delozier, Y.P. Sun, Y. Lin, Thermal conductivity of UltemTM/carbon nanofiller blends, High Perform. Polym. 18 (2006) 961–977, https://doi.org/10.1177/0954008306069133.
[62] K. Kalaitzidou, H. Fukushima, L.T. Drzal, Multifunctional polypropylene composites produced by incorporation of exfoliated graphite nanoplatelets, Carbon N Y 45 (2007) 1446–1452, https://doi.org/10.1016/j.carbon.2007.03.029.
[63] J. Li, J.K. Kim, M. Lung Sham, Conductive graphite nanoplatelet/epoxy nanocomposites: effects of exfoliation and UV/ozone treatment of graphite, Scr. Mater. 53 (2005) 235–240, https://doi.org/10.1016/j.scriptamat.2005.03.034.
[64] K. Kalaitzidou, H. Fukushima, H. Miyagawa, L.T. Drzal, Flexural and tensile moduli of polypropylene nanocomposites and comparison of experimental data to Halpin-Tsai and Tandon-Weng models, Polym. Eng. Sci. 47 (2007) 1796–1803, https://doi.org/10.1002/pen.20879.
[65] X. Jiang, L.T. Drzal, Multifunctional high density polyethylene nanocomposites produced by incorporation of exfoliated graphite nanoplatelets 1: morphology and mechanical properties, Polym. Compos. 31 (2010) 1091–1098, https://doi.org/10.1002/pc.20896.
[66] X. Sun, P. Ramesh, M.E. Itkis, E. Bekyarova, R.C. Haddon, Dependence of the thermal conductivity of two-dimensional graphite nanoplatelet-based composites on the nanoparticle size distribution, J. Phys. Condens. Matter 22 (2010), https://doi.org/10.1088/0953-8984/22/33/334216.
[67] L. Hu, T. Desai, P. Keblinski, Thermal transport in graphene-based nanocomposite, J. Appl. Phys. 110 (2011), https://doi.org/10.1063/1.3610386.
[68] M. Shtein, R. Nadiv, M. Buzaglo, K. Kahil, O. Regev, Thermally conductive graphene-polymer composites: size, percolation, and synergy effects, Chem. Mater. 27 (2015) 2100–2106, https://doi.org/10.1021/cm504550e.
[69] R.J. Young, M. Liu, I.A. Kinloch, S. Li, X. Zhao, C. Vallés, D.G. Papageorgiou, The mechanics of reinforcement of polymers by graphene nanoplatelets, Compos. Sci. Technol. 154 (2018) 110–116, https://doi.org/10.1016/j.compscitech.2017.11.007.
[70] K.P. Pramoda, H. Hussain, H.M. Koh, H.R. Tan, C.B. He, Covalent bonded polymer-graphene nanocomposites, J. Polym. Sci., Part A: Polym. Chem. 48 (2010) 4262–4267, https://doi.org/10.1002/pola.24212.
[71] J.N. Israelachvili, Intermolecular and Surface Forces, third ed., Academic Press, 2011.
[72] S. Vadukumpully, J. Paul, N. Mahanta, S. Valiyaveettil, Flexible conductive graphene/poly(vinyl chloride) composite thin films with high mechanical strength and thermal stability, Carbon N Y 49 (2011) 198–205, https://doi.org/10.1016/j.carbon.2010.09.004.
[73] E. Lago, P.S. Toth, G. Pugliese, V. Pellegrini, F. Bonaccorso, Solution blending preparation of polycarbonate/graphene composite: boosting the mechanical and electrical properties, RSC Adv. 6 (2016) 97931–97940, https://doi.org/10.1039/c6ra21962d.
[74] Z. Xu, C. Gao, In-situ polymerization approach to graphene-reinforced nylon-6 composites, Macromolecules 43 (2010) 6716–6723, https://doi.org/10.1021/ma1009337.
[75] H. Kim, C.W. Macosko, Processing-property relationships of polycarbonate/graphene composites, Polymer 50 (2009) 3797–3809, https://doi.org/10.1016/j.polymer.2009.05.038.
[76] H.-B. Zhang, W.-G. Zheng, Q. Yan, Y. Yang, J.-W. Wang, Z.-H. Lu, G.-Y. Ji, Z.-Z. Yu, Electrically conductive polyethylene terephthalate/graphene nanocomposites prepared by melt compounding, Polymer 51 (2010) 1191–1196, https://doi.org/10.1016/j.polymer.2010.01.027.
[77] K. Kalaitzidou, H. Fukushima, L.T. Drzal, A new compounding method for exfoliated graphite-polypropylene nanocomposites with enhanced flexural properties and lower percolation threshold, Compos. Sci. Technol. 67 (2007) 2045–2051, https://doi.org/10.1016/j.compscitech.2006.11.014.
[78] H. Kim, Y. Miura, C.W. Macosko, Graphene/Polyurethane nanocomposites for improved gas barrier and electrical conductivity, Chem. Mater. 22 (2010) 3441–3450, https://doi.org/10.1021/cm100477v.
[79] H. Kim, S. Kobayashi, M.A. AbdurRahim, M.J. Zhang, A. Khusainova, M.A. Hillmyer, A.A. Abdala, C.W. Macosko, Graphene/polyethylene nanocomposites: effect of polyethylene functionalisation and blending methods, Polymer 52 (2011) 1837–1846, https://doi.org/10.1016/j.polymer.2011.02.017.
[80] X.S. Du, M. Xiao, Y.Z. Meng, A.S. Hay, Facile synthesis of exfoliated and highly conductive poly(arylene disulfide)/graphite nanocomposites, Polym. Adv. Technol. 15 (2004) 320–323, https://doi.org/10.1002/pat.457.
[81] W.P. Wang, Y. Liu, X.X. Li, Y.Z. You, Synthesis and characteristics of poly(-methyl methacrylate)/expanded graphite nanocomposites, J. Appl. Polym. Sci. 100 (2006) 1427–1431, https://doi.org/10.1002/app.23471.
[82] A.A. Handlos, D.G. Baird, Processing and associated properties of in situ composites based on thermotropic liquid crystalline polymers and thermoplastics, J. Macromol. Sci., A: Polym. Rev. 35 (1995) 183–238, https://doi.org/10.1080/15321799508009637.
[83] S. Kim, I. Do, L.T. Drzal, Multifunctional xGnP/LLDPE nanocomposites prepared by solution compounding using various screw rotating systems, Macromol. Mater. Eng. 294 (2009) 196–205, https://doi.org/10.1002/mame.200800319.
[84] S.I. Marras, I. Zuburtikudis, C. Panayiotou, Solution casting versus melt compounding: effect of fabrication route on the structure and thermal behavior of poly(l-lactic acid) clay nanocomposites, J. Mater. Sci. (2010) 6474–6480, https://doi.org/10.1007/s10853-010-4735-6.
[85] E. Hammel, X. Tang, M. Trampert, T. Schmitt, K. Mauthner, A. Eder, P. Pötschke, Carbon nanofibers for composite applications, Carbon N Y (2004) 1153–1158, https://doi.org/10.1016/j.carbon.2003.12.043.
[86] H.R. Dennis, D.L. Hunter, D. Chang, S. Kim, J.L. White, J.W. Cho, D.R. Paul, Effect of melt processing conditions on the extent of exfoliation in organoclay-based nanocomposites, n.d. www.elsevier.com/locate/polymer.
[87] M. Tanahashi, Development of fabrication methods of filler/polymer nanocomposites: with focus on simple melt-compounding-based approach without surface modification of nanofillers, Materials 3 (2010) 1593–1619, https://doi.org/10.3390/ma3031593.
[88] J.W. Cho, D.R. Paul, Nylon 6 nanocomposites by melt compounding, n.d. www.elsevier.nl/locate/polymer.
[89] H.R. Dennis, D.L. Hunter, D. Chang, S. Kim, J.L. White, J.W. Cho, D.R. Paul, Effect of melt processing conditions on the extent of exfoliation in organoclay-based nanocomposites, n.d. www.elsevier.com/locate/polymer.
[90] J.T. Bendler, Handbook of Polycarbonate Science and Technology, Taylor & Francis, 1999. https://books.google.de/books?id=YL-cza_44N8C.
[91] D. Li, A.E. del Rio Castillo, H. Jussila, G. Ye, Z. Ren, J. Bai, X. Chen, H. Lipsanen, Z. Sun, F. Bonaccorso, Black phosphorus polycarbonate polymer composite for pulsed fibre lasers, Appl. Mater. Today 4 (2016) 17–23, https://doi.org/10.1016/j.apmt.2016.05.001.
[92] D. Freitag, G. Fengler, L. Morbitzer, Routes to New Aromatic Polycarbonates with Special Material Properties, n.d.
[93] V. Serini, Polycarbonates, in: Ullmann's Encyclopedia of Industrial Chemistry, Wiley-VCH Verlag GmbH & Co. KGaA, Weinheim, Germany, 2000, https://doi.org/10.1002/14356007.a21_207.
[94] A. Oyarzabal, A. Cristiano-Tassi, E. Laredo, D. Newman, A. Bello, A. Etxeberría, J.I. Eguiazabal, M. Zubitur, A. Mugica, A.J. Müller, Dielectric, mechanical and transport properties of bisphenol A polycarbonate/graphene nanocomposites prepared by melt blending, J. Appl. Polym. Sci. 134 (2017), https://doi.org/10.1002/app.44654.

[95] J.A. King, M.D. Via, F.A. Morrison, K.R. Wiese, E.A. Beach, M.J. Cieslinski, G.R. Bogucki, Characterisation of exfoliated graphite nanoplatelets/polycarbonate composites: electrical and thermal conductivity, and tensile, flexural, and rheological properties, J. Compos. Mater. 46 (2012) 1029–1039, https://doi.org/10.1177/0021998311414073.
[96] B. Shen, W. Zhai, M. Tao, D. Lu, W. Zheng, Enhanced interfacial interaction between polycarbonate and thermally reduced graphene induced by melt blending, Compos. Sci. Technol. 86 (2013) 109–116, https://doi.org/10.1016/j.compscitech.2013.07.007.
[97] T. Artham, M. Doble, Bisphenol A and metabolites released by biodegradation of polycarbonate in seawater, Environ. Chem. Lett. 10 (2012) 29–34, https://doi.org/10.1007/s10311-011-0324-4.
[98] N.H. Oberlies, C. Li, R.J. McGivney, F.Q. Alali, J.R. Tanner, J.O. Falkinham, Microbial-mediated release of bisphenol a from polycarbonate vessels, Lett. Appl. Microbiol. 46 (2008) 271–275, https://doi.org/10.1111/j.1472-765X.2007.02301.x.
[99] Jimmy T. Chow, Larry E. Erickson, Environmental Assessment for Bisphenol-A and Polycarbonate, 2007.
[100] J.F. Feller, A. Bourmaud, Rheological and calorimetric properties of recycled bisphenol A poly(carbonate), Polym. Degrad. Stabil. 82 (2003) 99–104, https://doi.org/10.1016/S0141-3910(03)00169-1.
[101] M.J. Reich, A.L. Woern, N.G. Tanikella, J.M. Pearce, Mechanical properties and applications of recycled polycarbonate particle material extrusion-based additive manufacturing, Materials 12 (2019), https://doi.org/10.3390/ma12101642.
[102] A.L. de la Colina Martínez, G. Martínez Barrera, C.E. Barrera Díaz, L.I. Ávila Córdoba, F. Ureña Núñez, D.J. Delgado Hernández, Recycled polycarbonate from electronic waste and its use in concrete: effect of irradiation, Construct. Build. Mater. 201 (2019) 778–785, https://doi.org/10.1016/j.conbuildmat.2018.12.147.
[103] D. Mahanta, S.A. Dayanidhi, S. Mohanty, S.K. Nayak, Mechanical, thermal, and morphological properties of recycled polycarbonate/recycled poly(acrylonitrile-butadiene-styrene) blend nanocomposites, Polym. Compos. 33 (2012) 2114–2124, https://doi.org/10.1002/pc.22342.
[104] C. Abeykoon, A. McMillan, C.H. Dasanayaka, X. Huang, P. Xu, Remanufacturing using end-of-life vehicles and electrical and electronic equipment polymer recyclates - a paradigm for assessing the value proposition, Int. J. Lightweight Mater. Manuf. 4 (2021) 434–448, https://doi.org/10.1016/j.ijlmm.2021.06.005.
[105] J. Datta, P. Kopczyńska, From polymer waste to potential main industrial products: actual state of recycling and recovering, Crit. Rev. Environ. Sci. Technol. 46 (2016) 905–946, https://doi.org/10.1080/10643389.2016.1180227.
[106] R. Liang, R.K. Gupta, The effect of residual impurities on the rheological and mechanical properties of engineering polymers separated from mixed plastics, n.d.
[107] A. Eddhahak, On a contribution to study some mechanical properties of WEEE recycled polymer blends, J. Appl. Polym. Sci. 138 (2021), https://doi.org/10.1002/app.51250.
[108] M. Taşdemir, D. Koçak, I. Usta, M. Akalin, N. Merdan, Properties of recycled polycarbonate/waste silk and cotton fiber polymer composites, Int. J. Polym. Mater. Polym. Biomater. 57 (2008) 797–805, https://doi.org/10.1080/00914030802089138.
[109] G. Japins, J. Zicans, R.M. Meri, T. Ivanova, R. Berzina, R. Maksimov, Recycled polycarbonate based nanocomposites, in: Key Engineering Materials, Trans Tech Publications Ltd, 2013, pp. 43–47, https://doi.org/10.4028/www.scientific.net/KEM.559.43.
[110] A. Al-Mulla, R.K. Gupta, Glass-Fiber reinforcement as a means of recycling polymers from post-consumer applications, J. Polym. Environ. 26 (2018) 191–199, https://doi.org/10.1007/s10924-017-0935-3.
[111] N.G. Karsli, T. Yilmaz, From polymeric waste to potential industrial product: modification of recycled polycarbonate, J. Elastomers Plastics 54 (2022) 857–876, https://doi.org/10.1177/00952443221087351.
[112] V. Lorenzo, M.U. de La Orden, C. Muñoz, C. Serrano, J. Martínez Urreaga, Mechanical characterisation of virgin and recovered polycarbonate based nanocomposites by means of Depth Sensing Indentation measurements, Eur. Polym. J. 55 (2014) 1–8, https://doi.org/10.1016/j.eurpolymj.2014.03.015.
[113] V. Chauhan, T. Kärki, J. Varis, Review of natural fiber-reinforced engineering plastic composites, their applications in the transportation sector and processing techniques, J. Thermoplast. Compos. Mater. 35 (2019) 1169–1209, https://doi.org/10.1177/0892705719889095.
[114] L. Botta, R. Scaffaro, F. Sutera, M.C. Mistretta, Reprocessing of PLA/graphene nanoplatelets nanocomposites, Polymers 10 (2018), https://doi.org/10.3390/polym10010018.
[115] S. Chatterjee, J.W. Wang, W.S. Kuo, N.H. Tai, C. Salzmann, W.L. Li, R. Hollertz, F.A. Nüesch, B.T.T. Chu, Mechanical reinforcement and thermal conductivity in expanded graphene nanoplatelets reinforced epoxy composites, Chem. Phys. Lett. 531 (2012) 6–10, https://doi.org/10.1016/j.cplett.2012.02.006.
[116] C. Vilaverde, R.M. Santos, M.C. Paiva, J.A. Covas, Dispersion and re-agglomeration of graphite nanoplates in polypropylene melts under controlled flow conditions, Compos. Appl. Sci. Manuf. 78 (2015) 143–151, https://doi.org/10.1016/j.compositesa.2015.08.010.
[117] F. Lin, Y. Xiang, H.S. Shen, Temperature dependent mechanical properties of graphene reinforced polymer nanocomposites – a molecular dynamics simulation, Compos. B Eng. 111 (2017) 261–269, https://doi.org/10.1016/j.compositesb.2016.12.004.
[118] R. Sun, L. Li, S. Zhao, C. Feng, S. Kitipornchai, J. Yang, Temperature-dependent mechanical properties of defective graphene reinforced polymer nanocomposite, Mech. Adv. Mater. Struct. 28 (2021) 1010–1019, https://doi.org/10.1080/15376494.2019.1625987.
[119] Y. Fan, Y. Xiang, H.-S. Shen, Temperature-dependent mechanical properties of graphene/Cu nanocomposites with in-plane negative Poisson's ratios, Research 2020 (2020) 1–12, https://doi.org/10.34133/2020/5618021.
[120] L. Shen, H.S. Shen, C.L. Zhang, Temperature-dependent elastic properties of single layer graphene sheets, Mater. Des. 31 (2010) 4445–4449, https://doi.org/10.1016/j.matdes.2010.04.016.
[121] Y.Y. Zhang, Y.T. Gu, Mechanical properties of graphene: effects of layer number, temperature and isotope, Comput. Mater. Sci. 71 (2013) 197–200, https://doi.org/10.1016/j.commatsci.2013.01.032.
[122] S.M. Liff, N. Kumar, G.H. McKinley, High-performance elastomeric nanocomposites via solvent-exchange processing, Nat. Mater. 6 (2007) 76–83, https://doi.org/10.1038/nmat1798.
[123] S. Araby, I. Zaman, Q. Meng, N. Kawashima, A. Michelmore, H.C. Kuan, P. Majewski, J. Ma, L. Zhang, Melt compounding with graphene to develop functional, high-performance elastomers, Nanotechnology 24 (2013), https://doi.org/10.1088/0957-4484/24/16/165601.
[124] K. Nawaz, U. Khan, N. Ul-Haq, P. May, A. O'Neill, J.N. Coleman, Observation of mechanical percolation in functionalised graphene oxide/elastomer composites, Carbon N Y 50 (2012) 4489–4494, https://doi.org/10.1016/j.carbon.2012.05.029.
[125] G. Ramorino, F. Bignotti, S. Pandini, T. Riccò, Mechanical reinforcement in natural rubber/organoclay nanocomposites, Compos. Sci. Technol. 69 (2009) 1206–1211, https://doi.org/10.1016/j.compscitech.2009.02.023.
[126] E. Guth, Theory of filler reinforcement, Rubber Chem. Technol. (1945) 596–604.
[127] S.C. Tjong, Structural and mechanical properties of polymer nanocomposites, Mater. Sci. Eng. R Rep. 53 (2006) 73–197, https://doi.org/10.1016/j.mser.2006.06.001.
[128] Y. Zhou, F. Pervin, L. Lewis, S. Jeelani, Experimental study on the thermal and mechanical properties of multi-walled carbon nanotube-reinforced epoxy, Mater. Sci. Eng. A 452–453 (2007) 657–664, https://doi.org/10.1016/j.msea.2006.11.066.
[129] Y.K. Choi, K.I. Sugimoto, S.M. Song, Y. Gotoh, Y. Ohkoshi, M. Endo, Mechanical and physical properties of epoxy composites reinforced by vapor grown carbon nanofibers, Carbon N Y 43 (2005) 2199–2208, https://doi.org/10.1016/j.carbon.2005.03.036.
[130] D.G. Papageorgiou, I.A. Kinloch, R.J. Young, Mechanical properties of graphene and graphene-based nanocomposites, Prog. Mater. Sci. 90 (2017) 75–127, https://doi.org/10.1016/j.pmatsci.2017.07.004.
[131] A. Allaoui, S. Bai, H.M. Cheng, J.B. Bai, Mechanical and electrical properties of a MWNT/epoxy composite, n.d. www.elsevier.com/locate/compscitech.
[132] B.S. Banerjee, S.S. Khaira, K. Balasubramanian, Thin film encapsulation of nano composites of polycarbonate (PC) for thermal management systems, RSC Adv. 4 (2014) 63380–63386, https://doi.org/10.1039/c4ra10183a.
[133] A. Al-Mulla, R.K. Gupta, C.W. John Zondlo, P.D. Charter D Stinespring, P.D. Hota V GangaRao, P.D. Carl Irwin, Glass Reinforcement of Recycled Polycarbonate, 2002.
[134] A. Al-Mulla, R.K. Gupta, Glass-Fiber reinforcement as a means of recycling polymers from post-consumer applications, J. Polym. Environ. 26 (2018) 191–199, https://doi.org/10.1007/s10924-017-0935-3.
[135] G. Abts, T. Eckel, R. Wehrmann, Polycarbonates, Ullmann's Encyclopedia of Industrial Chemistry, 2014.
[136] H. Yang, Z.S. Li, H.J. Qian, Y.B. Yang, X. bin Zhang, C.C. Sun, Molecular dynamics simulation studies of binary blend miscibility of poly (3-hydroxybutyrate) and poly(ethylene oxide), Polymer 45 (2004) 453–457, https://doi.org/10.1016/j.polymer.2003.11.021.
[137] T. Ramanathan, A.A. Abdala, S. Stankovich, D.A. Dikin, M. Herrera-Alonso, R.D. Piner, D.H. Adamson, H.C. Schniepp, X. Chen, R.S. Ruoff, S.T. Nguyen, I.A. Aksay, R.K. Prud'Homme, L.C. Brinson, Functionalised graphene sheets for polymer nanocomposites, Nat. Nanotechnol. 3 (2008) 327–331, https://doi.org/10.1038/nnano.2008.96.
[138] L. Botta, R. Scaffaro, F. Sutera, M.C. Mistretta, Reprocessing of PLA/graphene nanoplatelets nanocomposites, Polymers 10 (2018), https://doi.org/10.3390/polym10010018.
[139] D. Cho, S. Lee, G. Yang, H. Fukushima, L.T. Drzal, Dynamic mechanical and thermal properties of phenylethynyl-terminated polyimide composites reinforced with expanded graphite nanoplatelets, Macromol. Mater. Eng. 290 (2005) 179–187, https://doi.org/10.1002/mame.200400281.
[140] H. Ribeiro, W.M. Silva, M.T.F. Rodrigues, J.C. Neves, R. Paniago, C. Fantini, H.D.R. Calado, L.M. Seara, G.G. Silva, Glass transition improvement in epoxy/graphene composites, J. Mater. Sci. (2013) 7883–7892, https://doi.org/10.1007/s10853-013-7478-3.
[141] Y. zhen Sheng, H. Yang, J. yin Li, M. Sun, Predicting glass transition temperature of polyethylene/graphene nanocomposites by molecular dynamic simulation, Chem. Res. Chin. Univ. 29 (2013) 788–792, https://doi.org/10.1007/s40242-013-2443-x.
[142] R.P. White, J.E.G. Lipson, Polymer free volume and its connection to the glass transition, Macromolecules 49 (2016) 3987–4007, https://doi.org/10.1021/acs.macromol.6b00215.